Contrib Mineral Petrol (1983) 84:355–364

Contributions to Mineralogy and Petrology

Felsic mineral crystallization trends in differentiating alkaline basic magmas

C.M.B. Henderson[1] **and F.G.F. Gibb**[2]

[1] Department of Geology, The University, Manchester M13 9PL, UK
[2] Department of Geology, The University, Sheffield S1 3JD, UK

Abstract. Mineral compositional relationships have been studied in a variety of alkaline basic rocks from small, high-level intrusions. These small intrusions must have cooled quickly as the phases are all zoned, especially those forming the matrix of some of the rocks which seem to have formed under conditions of almost perfect fractional crystallization.

The compositions of nephelines from the various rocks define an overall evolutionary trend in which Na_2O, K_2O and CaO decrease and SiO_2 increases. The most SiO_2-rich nephelines plot in the nepheline plus feldspar stability field and must have crystallized metastably from the melt. Clear, interstitial analcime is definitely not a primary phase. It appears to be restricted to rocks which crystallized primary SiO_2-rich nepheline and formed from this phase by subsolidus recrystallization processes.

Most of the rocks studied appear to have crystallized plagioclase as the first felsic mineral. In some rocks this phase is zoned from $\sim An_{70-60}$, through anorthoclase compositions to rims of composition $\sim Or_{50}$ and this is the only feldspar present in the rocks. In other rocks the "plagioclase" shows zoning to similarly potassic compositions (Or_{40-50}) but this is accompanied by separate grains of orthoclase cryptoperthite. The zoning trends of the coexisting "plagioclase" and alkali feldspar allow the feldspar critical end point compositions to be estimated for these rocks. Rocks containing strongly zoned plagioclase as the only feldspar species are believed to have evolved towards relatively K_2O-rich low-temperature melting compositions due to the presence of mafic components.

The crystallization histories of the rocks are considered in terms of three planes in the An-Ne-Ks-Qz system i.e. Ne-Ks-Qz; $(Ne_{60}Ks_{40})$-An-Qz; and An-Ab-Or. Mineral and bulk rock compositional data together with textural criteria are used to modify phase equilibrium relations in these simple experimental systems to take account of the additional components (e.g. mafics) present in natural magmas.

1 Introduction

During a study of differentiated alkaline basic sills we became concerned with the problem of deducing the conditions of formation of the clear analcime occupying wedge-shaped interstices between plagioclase laths. Such analcime has frequently been interpreted as a primary phase (i.e. crystallized from the melt) even though experimental work shows that analcime only becomes a stable phase at temperatures well below the solidus of such rocks (Roux and Hamilton 1976). We have previously described textures in the Dippin sill crinanites showing alteration of a SiO_2-rich nepheline to clear analcime and concluded that the nepheline was a primary phase which altered to analcime during subsolidus interaction with deuteric and/or hydrothermal fluids (Henderson and Gibb 1977). In subsequent work we have found relics of similarly SiO_2-rich nepheline associated with interstitial analcime in a theralite from the Lugar sill, Ayrshire and Mohammed (1982) described the same association in rocks from the Eilean Mhuire sill, Shiant Isles.

There is little doubt that the nepheline described above is a late-crystallizing primary phase but the inter-relationships between the contemporaneous, late-crystallizing plagioclase, nepheline and possibly alkali feldspar are not clear. We therefore decided to study a selection of alkaline basic rocks, from a number of localities, which cover a considerable range of bulk composition (i.e. basicity and degree of undersaturation). The results of this work have further clarified the nepheline/analcime genetic relationship but are of wider importance in that the feldspar compositional trends present fascinating problems of interpretation. Thus the results have considerable significance in understanding felsic mineral crystallization trends in basic magmas undergoing strong fractionation.

2 Analytical methods

The felsic minerals were the principal subject of this work but mafic phases were also studied to establish the extent to which their presence would distort certain CIPW normative plots of the bulk rocks. Minerals were analysed using a Cameca Camebax electron microprobe fitted with a Link Systems 860-500 Energy Dispersive analytical system. A 15 kV accelerating voltage, 40° take-off angle, and 3nA incident beam current were used together with a defocussed beam (3–5 μm) to minimise alkali loss, especially from nepheline and analcime. Data were reduced using the Link System ZAF-4/FLS software. A presumed homogeneous nepheline from a nepheline syenite was also analysed to estimate the analytical precision and gave a mean composition (1 σ errors in brackets) of Ne 69.3 (0.7) Ks 16.3 (0.4) Qz 14.4 (1.0) (mol %). Rock analyses were obtained by XRF techniques using fused Li-borate glass discs.

Offprint requests to: C.M.B. Henderson

3 Results

The ranges of composition for the various minerals are given together with some essential petrographic information for each rock in the next section (3.1) and selected compositions are given in full in Table 1. The general mineral trends and their significance are discussed in sections 3.2 and 3.3. Only a representative selection of mineral analyses are plotted on Figs. 1 and 2 so that mineral trends for individual rocks are not obscured.

3.1 Petrographic notes and summary of essential mineral compositions

All the rocks chosen are from relatively small intrusions which must have cooled rapidly as indicated by their strongly zoned minerals. Accessory opaque oxides and apatite are ubiquitous as are secondary zeolites from the alteration of feldspar, nepheline, and analcime. In the following summaries maximum grain dimensions are noted, end-member mineral compositions are given as mol % and oxide values as w. %. Samples are numbered 1 to 12 and are identified with these numbers in the figures.

1) Olivine theralite, Otago, New Zealand (R 377). This rock is coarse grained with abundant, euhedral (possibly cumulus) titaniferous augite (2 mm, 50 vol. %) containing ~3.4% TiO_2 and ~9.6% Al_2O_3. Granular olivines ($1^1/_2$ mm, 3 vol. %) are zoned Fo_{68-56} and abundant plagioclase occurs as laths (6 mm) partially enclosing pyroxene. The plagioclase is strongly zoned, apparently continuously with no obvious core, from An_{68} through anorthoclase compositions, which are generally Ba-rich, to a sodic sanidine composition (Or_{49}) (see Table 1, analyses a–d). Nepheline forms fairly large patches (~3 mm) and appears to have started crystallizing soon after plagioclase. It varies in composition over the range $Qz_{14-23}Ne_{75-68}Ks_{11-9}$ with 1.4 to 0.8% CaO. Interstitial clear analcime is absent but feldspar and nepheline show some alteration to birefringent zeolites (having compositions similar to phillipsite and thomsonite).

2) Olivine theralite, Otago, New Zealand (R 378). This specimen is similar to number 1 except that it contains less pyroxene (6 mm, 27 vol. %). The pyroxene is sector zoned with TiO_2=2.7–4.7% and Al_2O_3=7.3–11.7% and has thin grey-green rims containing 1.0% TiO_2 and 2.1% Al_2O_3. Euhedral olivine (1 mm) is zoned Fo_{65-51} and plagioclase laths are small ($1^1/_2$ mm), not abundant and are often enclosed in large patches of nepheline (8 mm with individual subhedral grains ~2 mm). Plagioclase is zoned from $An_{79}Ab_{20.5}Or_{0.5}$ to $An_{24}Ab_{66}Or_8Cn_2$ and the nephelines are in the range $Qz_{12-19}Ne_{77-73}Ks_{11-8}$ averaging 1.0±0.2% CaO. Clear analcime is absent.

3) Crinanite, Madeira (MDG). Sample no. 3 contains subhedral olivines (2 mm, 8 vol. %) which are zoned Fo_{69-53}. Augite forms large interstitial and poikilitic crystals (7 mm) intergrown mainly with interlocking plagioclase laths (6 mm). This pyroxene is relatively unzoned (2.6% TiO_2, 4.5% Al_2O_3). The plagioclase grains have large, moderately homogeneous cores (~An_{65}) with rims zoned to An_{38}. These grains are commonly overgrown by thin rims of anorthoclase composition ($An_{20-9}Ab_{73-67}Or_{7-24}$; BaO

Table 1. Selected felsic mineral compositions

wt.%	Feldspars					Nephelines			Analcimes				
	(a)	(b)	(c)	(d)		(e)	(f)	(g)	(h)	(i)	(j)	(k)	
SiO_2	50.5	53.6	61.9	66.0		45.0	47.1	49.8	53.1	52.6	49.9	55.8	
Al_2O_3	31.5	29.7	24.2	19.8		32.8	32.8	30.9	25.6	25.1	25.6	23.2	
Fe_2O_3[a]	0.6	0.6	n.d.	n.d.		0.5	0.3	0.3	n.d.	n.d.	n.d.	n.d.	
CaO	14.4	11.8	4.9	0.9		2.5	1.1	0.6	1.4	1.4	3.4	0.6	
Na_2O	3.7	4.6	7.6	5.1		14.8	16.0	16.0	12.8	12.2	11.5	13.2	
K_2O	0.1	0.3	1.9	8.3		3.6	4.0	2.6	0.3	0.2	0.2	0.1	
BaO	n.d.	n.d.	1.4	n.d.		n.d.	n.d.	n.d.	n.d.	n.d.	n.d.	n.d.	
Total	100.8	100.6	101.9	100.1		99.2	101.3	100.2	93.2	91.6	90.6	93.0	
Cell formulae	8 (O)	8 (O)	8 (O)	8 (O)		8 (O)	8 (O)	8 (O)	6 (O)	6 (O)	6 (O)	6 (O)	
Si	2.29	2.41	2.73	2.96		2.15	2.19	2.31	1.92	1.94	1.87	2.01	
Al	1.68	1.58	1.26	1.05		1.85	1.80	1.69	1.09	1.09	1.13	0.99	
Fe^{3+}	0.02	0.02	–	–		0.02	0.01	0.01	–	–	–	–	
Ca	0.70	0.57	0.23	0.04		0.13	0.05	0.03	0.06	0.06	0.14	0.03	
Na	0.32	0.41	0.65	0.44		1.36	1.45	1.44	0.90	0.87	0.84	0.92	
K	0.01	0.02	0.11	0.48		0.22	0.24	0.15	0.01	0.01	0.01	0.01	
Ba	–	–	0.03	–		–	–	–	–	–	–	–	
Mol %													
An	67.8	57.4	22.8	4.6	An	6.4	2.4	1.3	3.1	2.9	7.9	1.3	An
Ab	31.5	41.1	64.2	45.9	Ne	67.6	67.6	63.6	49.1	46.4	48.3	46.3	Ne
Or	0.5	1.5	10.5	49.2	Ks	11.0	11.0	6.7	0.7	0.5	0.5	0.3	Ks
Cn (celsian)	0.0	0.0	2.5	0.3	Qz	15.0	19.0	28.4	47.1	50.2	43.3	52.1	Qz
Mol ratio 4Si/(Na+K+2Ca+Al)	–	–	–	–		–	–	–	3.73	3.71	3.31	4.10	4Si/(Na+K+2Ca+Al)

Key: (a)–(d) Feldspars from sample 1; *(b), (c)* and *(d)* are from the same zoned grain. *(e)* Nepheline, sample 10. *(f), (g)* Nepheline and *(h), (i)* clear analcime from sample 4. Analysis *(i)* has a 'fibrous' appearance and has *clearly* formed by alteration of nepheline. *(j)* Clear analcime from sample 6. *(k)* Clear analcime from sample 3

[a] Total Fe as Fe_2O_3

nd. = below 2 σ error

up to ~0.5%), which in turn may be overgrown by feldspar of composition $An_2Ab_{50}Or_{48}$. The anorthoclase and alkali feldspar zones form linings to the polygonal spaces between the interlocking plagioclase laths. These interstices are occupied by wedge-shaped grains of nepheline (1 mm), clear analcime and separate small alkali feldspar crystals (Or_{50}). Plagioclase/nepheline intergrowths occur rarely. The nephelines are in the compositional range $Qz_{16-22}Ne_{73-79}Ks_{11-9}$ (with 1.1 to 0.6% CaO) while the clear analcime is close to the stoichiometric composition ($NaAlSi_2O_6.H_2O$) after calculation of CaO (up to 0.6%) as anorthite (Table 1, analysis k).

4) Crinanite, Howford Bridge sill, Ayrshire, Scotland (12117). This rock is medium-grained with olivine (1 mm, 4 vol. %, Fo_{34-16}) set in a sub-ophitic intergrowth of pyroxene (3 mm, 30 vol. %) and plagioclase laths (2 mm). The pyroxene has pale pink cores (TiO_2=1.8%, Al_2O_3=4.4%) and thin greenish Fe-rich rims (TiO_2=0.7%, Al_2O_3=1.7%). The plagioclase is strongly zoned, apparently continuously, from $An_{63}Ab_{36.5}Or_{0.5}$ to $An_{13}Ab_{80}Or_{17}$. These grains have thin rims at least as potassic as $An_5Ab_{53}Or_{42}$. Small, apparently interstitial, grains vary from anorthoclase (Or_{15}) to sanidine (Or_{70}) compositions but are mostly in the range Or_{46-56}. The interstices are occupied by small amounts of clear analcime containing ~1.6% CaO, a more fibrous but still clear analcime which appears to have formed by alteration of nepheline, and very rare small relict nephelines (Table 1, analyses f to i). The full range of nepheline zoning is $Qz_{20-31}Ne_{69-62}Ks_{11-7}$ and 1.0 to 0.6% CaO.

5) Theralite, Lugar sill, Ayrshire, Scotland (L79/4). Minor amounts of zoned pyroxene and olivine phenocrysts occur in this rock and have compositional ranges TiO_2=4.1–0.8%, Al_2O_3= 7.9–2.4% and Fo_{88-59}, respectively. The matrix consists of granular pyroxene, biotite, plagioclase laths (1 mm), patches of clear analcime and rare nepheline and alkali feldspar. The plagioclase is zoned ($An_{74-17}Ab_{25.5-69}Or_{0.5-14}$), separate grains of alkali feldspar are ~$An_5Ab_{37}Or_{50}Cn_8$; nepheline is in the range $Qz_{25-28}Ne_{66-63}Ks_9$ (averaging 0.9±0.1% CaO) and clear analcime has ~0.3% CaO.

6) Essexite, Lennoxtown, Scotland (MV 13). In this rock pyroxene phenocrysts (6 mm, 27%) are concentrically and sector zoned averaging 2.3% TiO_2, 6.9% Al_2O_3. The groundmass pyroxene has a similar Fe/Mg ratio to the phenocrysts but lower TiO_2 (1.6%) and Al_2O_3 (2.6%) contents. Subhedral olivine phenocrysts (2 mm, 9 vol. %) have compositions in the range Fo_{70-62}. The groundmass contains matts of small plagioclase laths (1 mm) which are zoned, probably continuously, from $An_{68}Ab_{31}Or_1$, via anorthoclase ($An_{15}Ab_{63.5}Or_{19}Cn_{2.5}$) to at least $An_4Ab_{50}Or_{46}$. Rims of more K-rich feldspar (Or_{55}) occur on these plagioclases and there are also separate, small interstitial feldspar grains in the range $An_3Ab_{47-33}Or_{50-64}$. The interstices between the plagioclase laths also contain small amounts of nepheline (~$Qz_{27-32}Ne_{65-61}Ks_{8-7}$; CaO 1.0±0.1%) and clear analcime which is particularly rich in CaO, Al_2O_3 and poor in SiO_2 (see Table 1, analysis j). After recalculating CaO as anorthite the analcime is deficient in SiO_2 relative to the stoichiometric composition. Some grains of a more fibrous, isotropic analcime are relatively rich in both K_2O and CaO (~2.3% and ~2.1% respectively) with low analytical totals characteristic of hydrated zeolites. Such grains probably represent intermediate stages in the alteration of nepheline to analcime.

7) Essexite, Papeno Valley, Tahiti (1101). In this specimen euhedral pyroxenes (7 mm, 30 vol. %, ~3.9% TiO_2, ~7.8% Al_2O_3) occur as phenocrysts in a generally medium-grained matrix. Subhedral olivines (1 mm, Fo_{58}) occur in minor amounts. Plagioclase laths (up to 3 mm but generally much smaller) have fairly homogeneous cores with zoned margins (total range $An_{67}Ab_{31.5}Or_{1.5}$ to $An_{16}Ab_{67}Or_{17}$ with ~0.5% BaO). The interstices are occupied by abundant nepheline ($Qz_{16-23}Ne_{72-67}Ks_{12-10}$; 1.7–1.2% CaO) which also occurs (rarely) intergrown with the plagioclase. Alkali feldspar ($An_3Ab_{28-18}Or_{69-79}$; <0.5% BaO) is restricted to thin rims on, and intergrown with, the plagioclase/nepheline intergrowths. Clear analcime is present in very small amounts.

8) Teschenite, Salisbury Crags, Edinburgh, Scotland (B). This rock consists mainly of a relatively fine-grained intergrowth of pyroxene and feldspars; the latter show complex textural and compositional relations. Plagioclase is present as lath-shaped grains (1 mm) zoned from ~$An_{60}Ab_{39}Or_1$ to ~$An_{31}Ab_{63}Or_6$. These have quite thick ($^1/_2$ mm) overgrowths, usually untwinned, continuously zoned from ~$An_{25}Ab_{66}Or_9$ via anorthoclase compositions relatively rich in BaO (~1%) to rims as potassic as ~$An_3Ab_{53}Or_{44}$. These feldspars coexist with separate, small ($^1/_2$ mm) rectangular grains of simple twinned orthoclase cryptoperthite zoned from ~$An_2Ab_{48}Or_{50}$ at the centre to ~$An_3Ab_{57}Or_{40}$ at the rim. Also present are small amounts (<1%) of nepheline (not analyzed) and clear analcime (<0.6% CaO).

9) Theralite, Papeno Valley, Tahiti (1100). Sample 9 contains euhedral prismatic kaersutites (2 mm, 18 vol. %) which have TiO_2= 6.2–4.7%, Al_2O_3=13.9–12.4 and Na_2O=2.7–3.1%. Also present are small amounts of greenish augite ($1^1/_2$ mm, 3 vol. %) with 1.9% TiO_2, 5.3% Al_2O_3 and 1.7% Na_2O. Plagioclase laths (5 mm) have relatively homogeneous cores with zoned margins (total range $An_{64}Ab_{35}Or_1$ to $An_{44}Ab_{54}Or_2$). These often have thick rims of orthoclase cryptoperthite, the latter also occurring as interstitial grains (range $An_3Ab_{44-33}Or_{53-64}$; BaO up to ~1% but variable). Some interstitial regions are occupied by intergrowths of sericite and zeolites which possibly represent completely altered nephelines. No clear analcime is present.

10) Theralite, Papeno Valley, Tahiti (1104). This rock is similar to 9 mineralogically and texturally except that it is less mafic (8 vol. % kaersutite, $3^1/_2$% pyroxene) and that interstitial nepheline (5 mm) is present in substantial amounts. The plagioclase is zoned ($An_{61-22}Ab_{38-70}Or_{1-8}$) and the coexisting orthoclase cryptoperthite has compositions in the range $An_{1-4}Ab_{50.5-43}Or_{46-47}Cn_{2.5-6}$. Nepheline is in the range $Qz_{11-17}Ne_{76-72}Ks_{13-11}$ and is particularly CaO-rich (2.5 to 2.0% see table 1, analysis e). Nepheline/plagioclase and nepheline/alkali feldspar intergrowths are well developed. Clear analcime is absent.

11) Nepheline "dolerite", Loebauerberg, Germany (1762). In this so-called dolerite abundant euhedral pyroxene crystals (3 mm, 27 vol. %) are sector zoned (TiO_2=5.9–2.4%, Al_2O_3=9.8–4.1%) with thin green rims (TiO_2=2.7%, Al_2O_3=1.0%, Na_2O=7.7%). Abundant euhedral nepheline (2 mm) is in the range $Qz_{5-17}Ne_{79-70}Ks_{16-13}$ and containing 2.0 to 0.7% CaO. The cores of nephelines tend to have higher CaO contents than the rims and grains with the highest CaO tend to have the lowest SiO_2(Qz). The interstices between nephelines are occupied by intergrowths of radiating, birefringent Ca-rich zeolite (thomsonite?) and K-rich feldspar ($An_0Ab_{23}Or_{73-75.5}Cn_{4.0-1.5}$). Neither analcime nor plagioclase are present.

12) Nepheline "dolerite", Heidelberg, Germany (1789). The subhedral pyroxenes (5 mm, 21 vol. %) in this rock have inclusion-rich cores with TiO_2=2.2%; Al_2O_3=2.6%, Na_2O=1.7% and thin green rims which are Fe-rich with 3.1% TiO_2, 0.5% Al_2O_3, 8.0% Na_2O. Small euhedral olivines (<$^1/_2$ mm, 2 vol. %) occur with a composition Fo_{78}, while nepheline is abundant as subhedral grains ($Qz_{9-12}Ne_{73-70}Ks_{18}$) containing ~0.1% CaO. Patches of interstitial alkali feldspar ($An_{1-0.5}Ab_{20-11.5}Or_{71-87}Cn_{8-1}$) are intergrown with biotite and another felsic phase which has been completely replaced by fine-grained alteration products. Plagioclase and clear analcime are again absent.

3.2 Feldspar crystallization trends

The petrographic and mineral composition data summarised above can be used to divide the rocks into four groups:

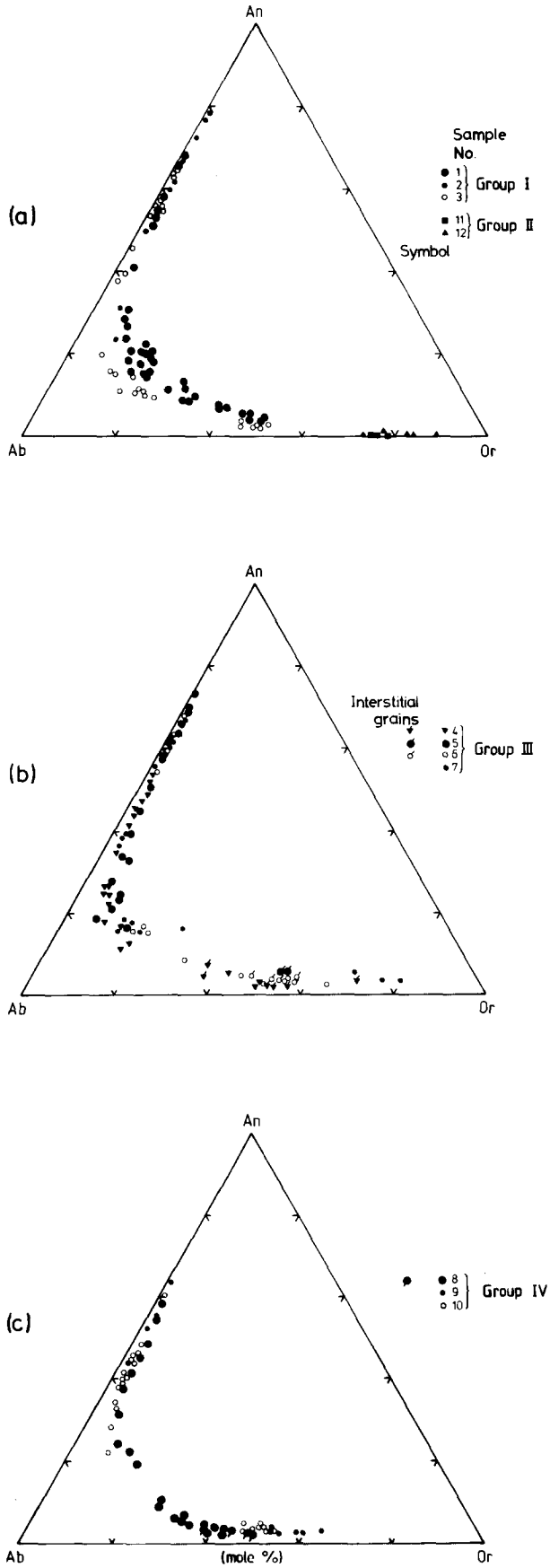

Fig. 1. Feldspar compositional trends (mol %). The symbols modified with a tick identify separate grains of alkali feldspar which are usually interstitial to zoned plagioclases

Group I: Rocks containing a single, strongly zoned, Ca-Na-K feldspar. For rocks in this group (samples 1, 2 and 3) the feldspar trend begins at very Ca-rich, K-poor plagioclase compositions which show (Fig. 1a) a gradual increase in Or as Ab increases to a maximum at 70 ± 5 after which Ab decreases rapidly as Or increases to a limit of $50 \pm 2\%$. This type of single "plagioclase" feldspar trend is especially well exhibited by the feldspars from sample 1 (larger solid circles in Fig. 1a). There is no doubt that the compositional variation over the range is essentially continuous; indeed a single grain in sample 1 shows a gradual change from $An_{57}Or_2$ via $An_{13}Or_{28}Cn_{2.5}$ to $Ab_{46}Or_{50}$ (see Table 1, analyses b, c, d). The feldspar compositions from this rock show some scatter in the anorthoclase range with particularly Ba-rich varieties (1–2% BaO) being displaced to slightly higher An and Or contents.

The feldspar trend for sample 3 covers the same overall range as for sample 1 but with compositional discontinuities (section 3.1) which occur within single crystals.

Group II: Rocks containing a single, zoned, K-rich feldspar. This group is typified by samples 11 and 12 (Fig. 1a). Although Ca-rich zeolites are present there is no evidence, textural or otherwise, that any of these could have formed by hydrothermal alteration of earlier plagioclase.

Group III: Two feldspar rocks with a discrete late-stage K-rich feldspar. This group is the least clear-cut of the four and includes samples 4, 5, 6 and 7 (Fig. 1b).

The bulk of the feldspars show a range of zoning similar to those in Group I. However, in addition to the fairly K-rich rims on plagioclase → anorthoclase cores, separate small interstitial grains of more K-rich feldspars are present (although sample 4 also has interstitial grains of more sodic compositions). Such interstitial grains are shown by a modified symbol in Fig. 1b. The very K-rich rims in samples 6 and 7 and separate grains of alkali feldspars with $Or > 50$ in all the rocks of this group are assumed to represent a late-crystallizing, K-rich second feldspar. Individual grains of interstitial alkali feldspar are too small and too restricted in composition to establish compositional trends with any certainty but we assume that there is an evolutionary trend from Or-rich to more Ab-rich ($\sim Or_{50}$) compositions.

Group IV: Rocks containing two feldspars from an early crystallization stage. Rocks 8, 9 and 10 belong to this category (Fig. 1c). The trend is unremarkable in that relatively calcic plagioclases crystallized together with K-rich alkali feldspars from an early stage. However, the compositional trends for the coexisting feldspars in sample 8 are highly significant in that their zoning trends meet at a composition of $\sim An_3Ab_{55}Or_{42}$. This must represent the composition of the critical end point on the feldspar solvus/solidus intersection for sample 8 (see section 4.3).

Clearly the bulk compositions of the parental magmas were crucial in controlling the feldspar crystallization trends. In addition, the extreme zoning suggests that (at least in the final stages) the crystallization may have been close to perfect fractionation. The remarkable feature common to the rocks of Groups I, III and IV is that the plagioclase-anorthoclase-sodic sanidine trend shows a far greater enrichment in K than is normally found (or expected). This is discussed further below (section 4).

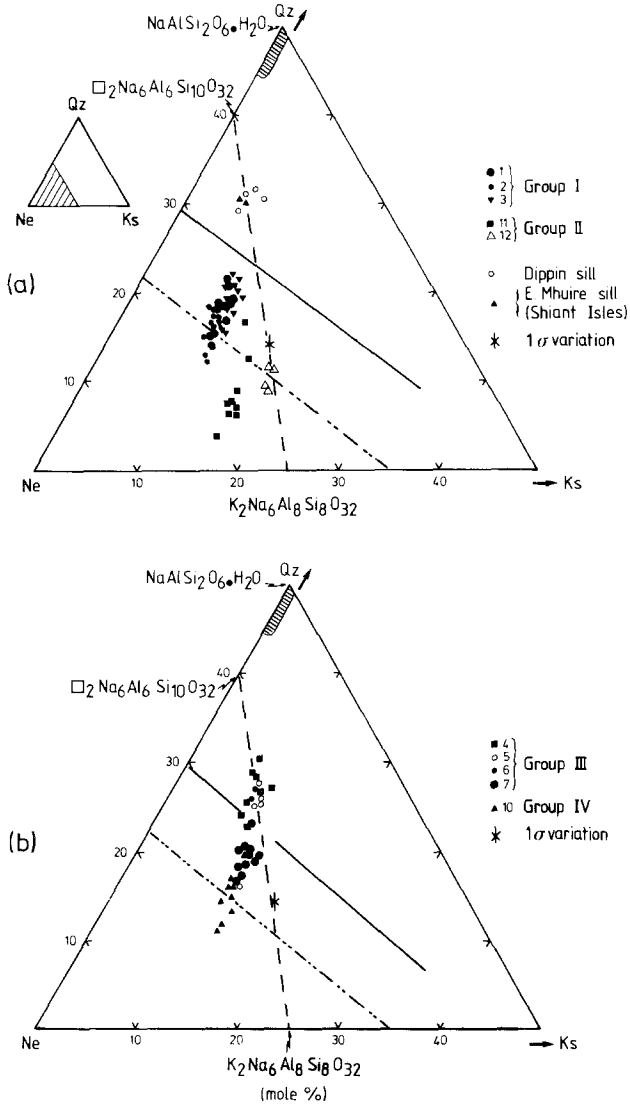

Fig. 2. Nepheline compositional relations (mol %). The dashed line denotes the Dollase and Thomas (1978) nepheline trend. The solid line marks the maximum limit for solid solution of feldspar in nepheline at 1,068° C, 1 atm. This is extrapolated from the limit in the binary Ne-Qz system (Greig and Barth 1938). The dash-two dot line marks the limit of solid solution at 700° C, 1 kbar P_{H_2O} (Hamilton 1961). The shaded area near the stoichiometric analcime composition covers the range of analcime compositions observed in this work

3.3 Nepheline crystallization trends

The rocks vary from those which crystallized abundant nepheline from a very early stage (e.g. samples 11, 12), to those which crystallized only small amounts of nepheline during the final stages of solidification (e.g. samples 4, 5, 6, 8; crinanites from the Dippin and Shiant Isles sills are also in this category). Other samples crystallized nepheline at an intermediate stage between these extremes (e.g. samples 1, 2, 3, 7, 9, 10). In addition, some of the rocks (e.g. samples 3, 7, 10) contain rare nepheline/plagioclase intergrowths suggesting the possibility of a reaction relationship between these phases (cf. Henderson and Gibb 1972).

The compositional trends of nephelines from all of the samples overlap to give an overall trend in which Ne and Ks components decrease as Qz increases (Fig. 2). Also included in Fig. 2 are the compositions of nephelines from the Dippin Sill, Arran (Gibb and Henderson 1978) and the Eilean Mhuire sill, Shiant Isles (Mohammed 1982). The nepheline compositions for different samples appear to be related to the amount and time of nepheline crystallization. Thus, nephelines in samples 11 and 12 (early crystallization) tend to have the lowest Qz contents. In addition, these nephelines coexist with K-rich feldspar (Group II) and are the most potassic varieties encountered in this study. Where small amounts of nepheline crystallized very late in the fractionation process these are relatively rich in Qz (e.g. samples 4, 5, 6, Dippin and Eilean Mhuire sills). Nepheline crystallizing under intermediate conditions tend to have intermediate Qz contents (samples 1, 2, 3, 7, 10).

Many of the interstitial nepheline grains analysed are too small to relate compositional trends unequivocally to sequence of crystallization but rocks with larger euhedral grains (e.g. sample 11) tend to have nephelines with more Ca-rich cores and less Ca-rich rims. In addition, the nephelines in several of the samples show an inverse relationship between CaO and SiO_2 enrichment (e.g. sample 4). Thus it seems likely that, in a given rock, early crystallized nephelines are relatively rich in An, Ne, Ks and poor in Qz while the opposite is true for later varieties. This suggestion is supported by the rims of nepheline phenocrysts from phonolites being enriched in SiO_2 relative to their cores (Tilley 1959; Brown 1970). This trend of increasing Qz component might be expected during magmatic crystallization of nepheline on its own but when this is joined by feldspar the nepheline should become saturated with feldspar components (i.e. saturated with Qz). Further crystallization under equilibrium conditions might be expected to produce nephelines with increasing Ks and decreasing Qz contents (Hamilton 1961).

The situation is further complicated by the most SiO_2-rich nephelines having compositions falling in the stability field of nepheline plus feldspar in the Ne-Ks-Qz system (Hamilton 1961). The extent of solid solution of feldspar in nepheline will, of course, depend on T and P but the maximum limit should be close to the 1068° C line in Fig. 2. This limit is extrapolated from the 1 atm Ne-Ab system (Greig and Barth 1938) but the presence of water under pressure should decrease both the temperature and the solid solution limit (cf. the limit for 700° C in Fig. 2). Thus it seems that the nepheline trend described here extends outside the nepheline stability field.

Dollase and Thomas (1978) described a nepheline trend falling between end members $K_2Na_6Al_8Si_8O_{32}$ and $\square_2Na_6Al_6Si_{10}O_{32}$ ($\square$ = cavity cation vacancy) (Fig. 2). Dollase and Thomas suggested that this trend was controlled by the strong site preference which led to the smaller cation site being filled with Na (and Ca) with the larger site containing K or being vacant. The nepheline compositions described here are generally CaO-rich with the sum of Na + Ca [for 32 (O)] averaging 6.1 ± 0.1. Consequently, although our nephelines plot close to the Dollase and Thomas trend they seem to be displaced to more Ne-rich compositions at low Qz contents. However, the natural nephelines considered by Dollase and Thomas are all from syenitic rocks and presumably coexist with potassic alkali feldspars rather than relatively sodic feldspars as in this study. In this respect it is significant that the nepheline from sample 12 coexists with abundant K-rich feldspar and plots closer to Dollase and Thomas' trend than the nephelines from any of the

other samples analysed. The implication of these relationships is that the strong site preference discussed by Dollase and Thomas may allow the metastable crystallization of SiO_2-rich nephelines (i.e. $\gtrsim 23$ mol% Qz) under conditions of strong fractionation due to rapid cooling.

3.4 Composition and origin of clear analcime

The CaO contents of the clear, interstitial analcimes from different rocks are rather variable. Those with high CaO have high Al_2O_3 and low Na_2O and SiO_2 contents (e.g. Table 1, analysis j). After recalculation of CaO as anorthite, these analcimes show relatively low Ne contents and 4Si/(Na+K+2Ca+Al) mole ratios (Table 1) and plot at the SiO_2-poor end of the analcime composition range (shown as the shaded areas in Figs. 2a and b) i.e. they show solid solution towards natrolite (Saha 1959). These SiO_2-poor analcimes have Ne:Qz ratios similar to those having the highest thermal stability under both subsolidus and liquidus conditions (Kim and Burley 1971; Roux and Hamilton 1976).

Interstitial clear analcimes with intermediate CaO contents (e.g. Table 1, analyses h and i) are slightly more SiO_2-rich and have higher 4Si/(Na+K+2Ca+Al) ratios while those with the lowest CaO contents (e.g. Table 1, analysis k) have the lowest Al_2O_3 and highest Na_2O and SiO_2 contents. These latter analcimes, after recalculation of CaO as anorthite, plot close to the stoichiometric composition (Fig. 2). It seems likely that the most SiO_2-poor, CaO-rich analcimes represent the original analcimes to form in these rocks (Gibb and Henderson 1978) and that recrystallization of these, at lower temperatures, tends to produce lower CaO, more SiO_2-rich varieties. Indeed, some rocks contain another variety of analcime which is slightly brownish and is closely associated with other zeolites. This analcime has very low CaO, has a stoichiometric composition ($NaAlSi_2O_6 \cdot H_2O$) and undoubtedly forms later in the history of the rock than the clear variety.

Clear interstitial analcime is absent from rocks which crystallized abundant nepheline from an early stage (e.g. samples 1, 2, 9, 10, 11, 12) even though abundant late-stage zeolites may be present. Such rocks tend to contain relatively SiO_2-poor nepheline which does not seem to be susceptible to alteration to the clear analcime. In contrast, rocks that crystallised SiO_2-rich nepheline late in the fractionation process have ubiquitous clear analcime. Such SiO_2-rich nephelines are likely to have crystallized metastably from the melt (see above). At lower temperatures, in the presence of water, these nephelines must have been highly unstable and usually show clear textural evidence of very advanced conversion to clear analcime such that in some rocks relict SiO_2-rich nepheline is *extremely* rare.

It is interesting to note that extrapolation of the compositional trend (Fig. 2) for the nephelines analysed in this study would give an intersection on the Ne-Qz join close to the compositions of the most SiO_2-poor analcimes. This compositional relationship is consistent with our suggestion that analcime forms from SiO_2-rich nepheline. The fact that there is a small gap between the compositions of the most SiO_2-rich nephelines and the most SiO_2-poor analcimes could simply reflect the extreme instability of the former i.e. such compositions would have been completely converted to analcime. Thus it seems that our previous suggestions (Henderson and Gibb 1977) about the way in which clear, interstitial analcime formed are essentially confirmed. However, we can now add that the high-SiO_2 nepheline → analcime reaction may be almost isochemical and not require the participation of sodic plagioclase or alkali feldspar.

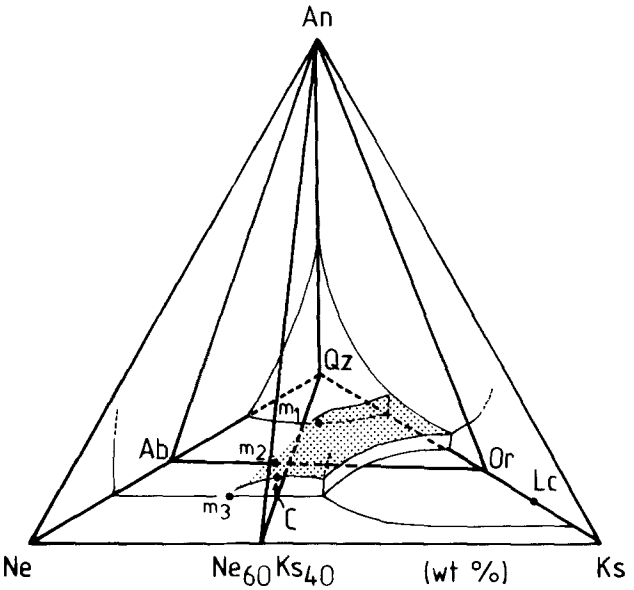

Fig. 3. Schematic phase relations for the An-Ne-Ks-Qz system at 1 kbar P_{H_2O} (after MacKenzie 1972 and Norris 1973). The stippled area represents the two-feldspar surface. m_1, m_2, and m_3 mark the "granite", feldspar and "phonolite" minimum compositions. C marks the intersection of the plagioclase-alkali feldspar-nepheline field boundary with the plane ($Ne_{60}Ks_{40}$)-An-Qz

4 Rock compositions and felsic mineral crystallization trends

Before the significance of the different feldspar crystallization trends can be fully evaluated it is essential to consider the bulk rock compositions (parent liquids?) in terms of phase relations in the system An-Ne-Ks-Qz or as projections onto planes within this system.

Many of the samples studied show evidence of early crystallization and possibly accumulation of Al_2O_3-rich titanaugite and/or kaersutite (section 3.1). The crystallization of such phases will distort the CIPW normative plots onto An-Ab-Or and Ne-Ks-Qz planes – in particular the very high Al_2O_3 contents of augite ($\sim 11\% Al_2O_3$) will substantially increase normative *an*. We have therefore used modal and analytical data to recalculate the bulk rock compositions minus pyroxene and amphibole. The parent liquid compositions controlling felsic mineral phase relations are assumed to be close to the rock compositions recalculated minus mafics. One other correction is necessary before highly SiO_2-undersaturated compositions can be usefully plotted in An-Ab-Or. The CIPW norm calculates *ne* as the pure Na-component rather than as the naturally occurring K-bearing compositions. We have chosen to avoid the consequent distortion by recalculating all *ne* as *ab* i.e. this is equivalent to projecting from the undersaturated field in An-Ne-Ks-Qz towards the Qz apex. The normative compositions recalculated in the above manner are believed to represent possible liquids which fractionated to give the observed mineral compositional trends.

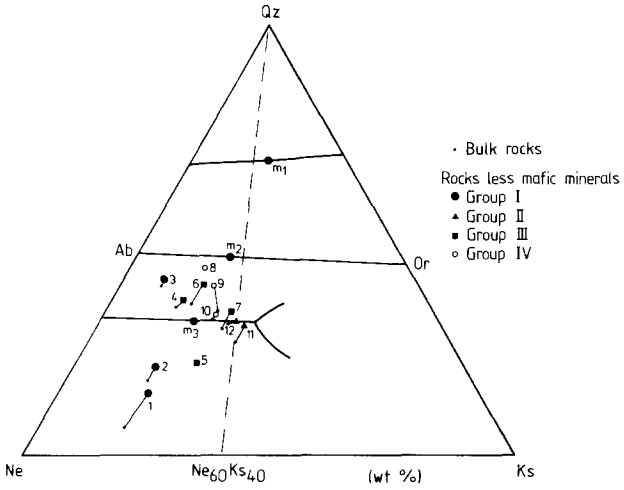

Fig. 4. Phase relations for the system Ne-Ks-Qz at 1000 bars P_{H_2O} (after Hamilton and MacKenzie 1965). Also shown are the projected normative compositions for the bulk rocks and the rock compositions corrected for mafic components. The sample numbers are identified in the text

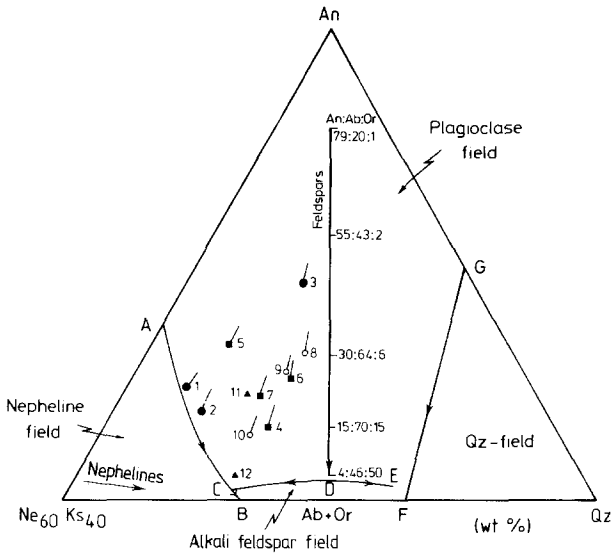

Fig. 5. Schematic phase relations for the ($Ne_{60}Ks_{40}$)-An-Qz plane through the An-Ne-Ks-Qz system. Generalized nepheline and feldspar compositional trends are shown. Rock compositions minus mafic components are plotted (symbols as in Fig. 4). For further explanation see text

We have considered the rock data projected onto three planes in the quaternary felsic system An-Ne-Ks-Qz (Figure 3): Ne-Ks-Qz; ($Ne_{60}Ks_{40}$)-An-Qz; and An-Ab-Or.

4.1 The residua system Ne-Ks-Qz

The 1000 bar P_{H_2O} phase relations in the Ne-Ks-Qz system (Hamilton and MacKenzie 1965) are shown in Fig. 4. Perfect fractional crystallization of liquids plotting on the Ab-Or join will give final liquids and feldspars having the compositions of the binary minimum (m_2) i.e. Or_{35}. Oversaturated liquids will fractionate to the "granite" minimum (m_1) and the final feldspar will have the alkali ratio appropriate to m_1 (i.e. feldspar composition $\sim Or_{50}$). In contrast, undersaturated liquids will fractionate to the "phonolite" minimum (m_3) and the final feldspar will have a composition of $\sim Or_{35-38}$ based on the form of the unique fractionation curve postulated by Hamilton and MacKenzie (1965). This latter composition is significantly less potassic than observed in our group I feldspar trend.

The bulk rocks and recalculated rock compositions are also plotted in Fig. 4. The compositions project into either the primary phase field of feldspar or nepheline. However, it is misleading to consider their crystallization behaviour in this plane because the An component substantially affects the phase relations as can be shown using another projection in An-Ne-Ks-Qz (Fig. 3), namely ($Ne_{60}Ks_{40}$)-An-Qz.

4.2 ($Ne_{60}Ks_{40}$)-An-Qz

The position of this plane is shown by heavy lines in Fig. 3. This plane is sufficiently potassic to intersect the two-feldspar surface in the An-Ne-Ks-Qz system (Fig. 3, stippled surface). More-sodic compositional planes would not intersect this surface and more-potassic planes would intersect the leucite field – the latter can be ignored since none of the rocks studied crystallized leucite.

The phase relationships for the plane chosen are shown schematically in Fig. 5. Note that, for the compositional plane considered, the two feldspar boundary does not intersect the quartz field for low-pressure conditions – it is drawn terminating at E. A thermal maximum on the two feldspar surface is shown at D. C is *not* an invariant point, it is a piercing point for the plagioclase-alkali feldspar-nepheline field boundary (see Fig. 3).

The recalculated rock compositions are shown in Fig. 5 together with possible feldspar and nepheline crystallization trends (e.g. for group I rocks – see Fig. 1a). A short tie line is drawn from each recalculated rock composition towards the most calcic plagioclase composition observed in that rock. This composition represents the *minimum* An content of the first plagioclase for each rock and gives some idea of the early evolutionary trends for liquids crystallizing plagioclase as the first felsic phase.

Samples 1 and 2 show textural evidence that plagioclase crystallized as the first felsic mineral but that this was soon joined by nepheline. Thus the nepheline/plagioclase field boundary has been drawn close to, but on the Ne-rich side of, these rock compositions. The boundary so drawn is displaced to more Ne-rich compositions relative to that for the An-Ne-Qz system at 1 atm (Schairer 1957). Samples 11 and 12 show clear evidence that nepheline crystallized early – the plot of 12 is just outside the nepheline field but sample 11 is displaced to anomalously high An contents because of the presence of abundant, late-stage Ca-rich zeolite. The other samples fall well inside the plagioclase field and clearly crystallized substantial amounts of plagioclase as the first felsic mineral.

Textural evidence shows that samples 8, 9 and 10 (group IV) undoubtedly crystallized alkali feldspar before nepheline and presumably their evolving liquid compositions intersected the two-feldspar boundary somewhere to the left of D. The plagioclase tie-line orientation for samples 8 and 9 are consistent with intersection between D and C but the intersection for sample 10 is less clear-cut. These rela-

tionships again suggest that the nepheline field is slightly smaller than in the An-Ne-Qz system and the two-feldspar field boundary is extended to more Ne-rich compositions to intersect the nepheline feldspar boundary at C.

Samples 3, 7 and 10 show textures consistent with plagioclase and nepheline having a reaction relationship. Thus the nepheline-plagioclase boundary (Fig. 5, AC) must change from a coprecipitation to a reaction boundary before C is reached. The piercing point C (i.e. the projection of the plagioclase-alkali feldspar-nepheline field boundary) is therefore, likely to be a reaction point and the arrow on the boundary CB is drawn pointing towards B to be consistent with this suggestion.

There is no unequivocal textural evidence for the rocks of Group III indicating whether nepheline or alkali feldspar crystallized as the second felsic phase. However, the recalculated rock data and their associated Ca-rich plagioclase tie lines suggest that only sample 5 crystallized nepheline while samples 4, 6 and 7 crystallized alkali feldspar as the second phases. It is essential to note that the projection used in Fig. 5 does not show the importance of the rock K/Na ratio in controlling whether only one feldspar will crystallize (e.g. samples 1, 2, 3, 11 and 12) or whether two will form – the An-Ab-Or projection will be used to discuss this relationship.

The contraction of the nepheline field mentioned above is presumably due to the presence of mafic components. The 1 atm phase relations for the systems Fo-Ne-SiO_2 (Schairer and Yoder 1961), Fa-Ne-SiO_2 (Bowen and Schairer 1938) and Di-Ne-SiO_2 (Schairer and Yoder 1960) support this prediction as the mafic components all decrease the nepheline field in favour of the mafic and feldspar phases.

4.3 An-Ab-Or

The phase relations in the An-Ab-Or plane (see Fig. 3) are shown schematically in Fig. 6 together with the bulk rock and recalculated rock compositions projected onto the plane. AC represents the trace of the two-feldspar surface and XKZ a possible polythermal intersection of solidus and solvus surfaces for the generalized conditions of crystallization of the rocks currently being studied. The latter curve was drawn to include as many as possible of the recalculated Group I and II compositions in the one-feldspar field and of the Group III and IV compositions in the two-feldspar field. Only two samples plot in the "wrong" fields. The corrected composition for sample 4 plots in the one-feldspar field suggesting that too much early crystallized pyroxene may have been subtracted in the recalculation. Sample 11 falls in the two-feldspar field because of the presence of substantial amounts of late-stage Ca-zeolite (see above).

The crystallization of the rock compositions can be discussed in the light of the feldspar compositional trends described earlier (section 3.2, Figs. 1a, b, c). Generalized feldspar trends are shown in Fig. 6: DEFG represents the single feldspar trend of Group I and the main feldspar trend in Group III; HJL the potassic feldspar trends for Groups II and III. Group IV rocks have a plagioclase-anorthoclase trend from D to F and a coexisting alkali feldspar trend from J extended to F.

Most of the rock and feldspar data for the different Groups (section 3.2) are compatible with phase relations expected for An-Ab-Or although several aspects require

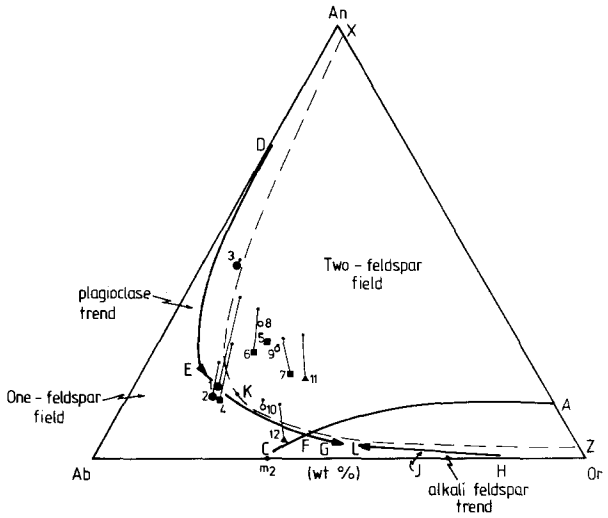

Fig. 6. Schematic phase relations for the An-Ab-Or system. AC is the feldspar field boundary, XKZ the intersection of the solidus and the solvus separating the two-feldspar and one-feldspar fields. DEFG and HJL represent the generalized "plagioclase" and alkali feldspar compositional trends. Bulk rocks and rock compositions minus mafic components are plotted (symbols as in Fig. 4). For further explanation see text

further comment. It seems surprising that sample 2 contains plagioclase more An-rich than the more-calcic sample 3. However, it is likely that the large, relatively homogeneous, plagioclase cores in sample 3 formed under equilibrium conditions (i.e. complete reaction of the most Ca-rich first crystallizing plagioclase) while the plagioclase in sample 2 formed under fractional crystallization conditions from an early stage.

The main problem in understanding the feldspar trend for Group I (e.g. samples 1, 2, 3) is to explain how the feldspar became zoned to compositions as potassic as Or_{50} (section 3.2). Further consideration of the phase relations in An-Ab-Or is necessary. Ca-rich liquids with bulk compositions plotting in the two-feldspar field (e.g. Group IV) will crystallize An-rich plagioclase initially, the liquid will intersect the two-feldspar boundary somewhere along AC (Fig. 6) and alkali feldspar will then crystallize. The zoning patterns for the two coexisting feldspars in sample 8 (Group IV) indicate that, under fractional crystallization conditions, the two feldspars crystallized side-by-side down to the solidus. Thus, for sample 8 at least, AC represents a coprecipitation boundary for the whole of its length. In this case, for perfect fractional crystallization, liquids lying on AC would trend to C and plagioclase and alkali feldspar compositions would trend towards the critical end point (K) on the solidus-solvus intersection. Tuttle and Bowen (1958) and Carmichael et al. (1974) assumed that the composition of point K was in the anorthoclase compositional range i.e. more sodic than the coexisting liquid. However, Stewart and Roseboom (1962) considered the various possibilities for the termination of the two-feldspar boundary in An-Ab-Or. They stressed that different terminations may arise depending either on the presence of additional components in the liquids or on differences in total pressure. Indeed two of the possible terminations (Stewart and Roseboom cases D and E, pp. 300 and 301) have critical end point compositions more potassic than the associated liquid on the field boundary. Thus the presence of excess Qz,

Ne + Ks, or mafic components in natural magmas may be associated with more potassic critical end points for the ternary feldspar composition. Indeed, the feldspar data reported here suggest critical end point compositions $\sim An_3Ab_{47}Or_{50}$ for samples 4 and 6 (Group III) and $\sim An_3Ab_{55}Or_{42}$ for sample 8 (Group IV). These compositions are significantly more potassic than the critical solution curve defined by Parsons and Brown (1983) and this will be considered further in another publication (Henderson, in prep.). However, it seems likely that the group I rock liquids can never have intersected the two-feldspar boundary and thus the critical end point composition cannot be the controlling factor for the group I feldspar trend.

Assuming perfect fractionation, for liquid compositions exactly on the An-Ab-Or plane, Ca-rich liquids in the one-feldspar field (e.g. point 3, Fig. 6) will fractionate towards the binary minimum (m_2, Fig. 6). The final feldspar will have the same composition as the last liquid i.e. $\sim Or_{35}$at low P_{H_2O}. The compositional relations become more complex for compositions either over-or undersaturated in SiO_2 relative to this plane. Thus in the An-Ne-Ks-Qz system Ca-bearing oversaturated liquids will fractionate towards the "granite" minimum. Feldspars will be zoned from Ca-rich cores to rims having the approximate composition Or_{50} (see section 4.1). In contrast, Ca-bearing undersaturated liquids in the An-Ne-Ks-Qz system will fractionate towards the "phonolite" minimum. Feldspars will again be zoned from relatively Ca-rich plagioclase cores to rims of composition close to $\sim Or_{35-38}$ (see section 4.1) i.e. less potassic than found for Group I samples.

The trends predicted above assume that the minima in the Ne-Ks-Qz system control the final stages of crystallization of more complex natural melts. There is little reason to believe that the An-component significantly affects the compositions of the final liquids fractionated from sodic bulk compositions plotting in the one-feldspar field of An-Ne-Ks-Qz (i.e. liquids that do not intersect the two-feldspar field boundary). However, there is good evidence that the phase relations are modified for *peralkaline* liquids (Thompson and MacKenzie 1967; Nash et al. 1969; Carmichael et al. 1974). Indeed Carmichael (1964) showed that feldspar phenocryst, groundmass feldspar and rock compositions for kenytes suggested an effective minimum composition more potassic than the "phonolite" minimum in Ne-Ks-Qz. There is no hint of peralkalinity in our samples but it is possible that the mafic components have a similar effect. Thus a sufficiently large displacement of the undersaturated minimum melting composition towards more potassic compositions could explain the extension of our Group I trend to K-rich feldspar compositions up to $\sim Or_{50}$.

Finally, it is interesting to consider whether the single-feldspar, group I trend is restricted to *undersaturated* magmas. With regard to this, it may be significant that the plagioclase compositional trend observed in the *tholeiitic* Picture Gorge basalt (Lindsley and Smith 1971) extends from $\sim An_{85}$, via $\sim An_{15}Or_{15}$ to $\sim Or_{55}$; i.e. almost identical to our Group I trend. Morse (1980) discussed this Picture Gorge trend and suggested that it is a single feldspar trend which formed by fractional crystallization of liquids which followed an evolutionary path very close to that of the zoned feldspars. Morse concluded that "the end of the process is assumed to occur when the liquid and feldspar both reach a minimum on or near the Ab-Or join". However, although there can be little doubt that the relevant minimum will have very little of the An component it seems likely that the last liquid for tholeiitic basalt will evolve towards the "granite" rather than the feldspar minimum. It seems clear that the additional chemical components (e.g. Qz, Di, Hy) present in the tholeiitic Picture Gorge magma modify the phase relations so as to allow the plagioclases to become more potassic than the binary minimum composition. Thus the trend to potassic rims on zoned plagioclase-anorthoclase cores (e.g. Picture Gorge and our Group I trends) may be a feature of highly fractionated, low-K basaltic magmas in general rather than of alkali basaltic magmas alone.

Conclusions

1. Nephelines from strongly fractionated alkaline basic igneous rocks define overlapping evolutionary trends from $\sim Qz_4Ne_{80}Ks_{16}$ to $\sim Qz_{32}Ne_{62}Ks_6$ (mol%). The CaO contents of nephelines from different rocks are variable but there is a tendency for CaO to decrease with fractionation e.g. (CaO 2.0–0.7 wt.%; An5.3–1.6 mol %). The most SiO_2-rich nephelines plot in the stability field of nepheline plus albite and are believed to have crystallized metastably from the melt under conditions of extreme fractionation during the final stages of crystallization.
2. Clear, interstitial analcime initially forms with a relatively CaO-rich, SiO_2-poor composition by low-temperature alteration of primary SiO_2-rich nepheline. This analcime may recrystallize at lower temperatures to give a virtually CaO-free, stoichiometric composition, sometimes associated with other zeolites.
3. The feldspars in the rocks studied generally show extreme compositional zoning. Rocks with relatively K_2O-rich bulk composition crystallized two coexisting feldspars (Groups III and IV). One such rock (sample 8) contains one feldspar zoned from plagioclase $\sim An_{60}$, through anorthoclase compositions to $\sim An_3Ab_{53}Or_{44}$ together with separate grains of alkali feldspar zoned from $\sim An_2Ab_{48}Or_{50}$ to $\sim An_3Ab_{57}Or_{40}$. The fact that the margins of both feldspars have the same rim compositions, within experimental error, indicates that the final stages of crystallization were close to perfect fractionation. The feldspar critical end point for this rock appears to be at a composition of $An_{3\pm1}Ab_{55\pm2}Or_{42\pm2}$. Other slightly more basic bulk compositions (e.g. samples 4 and 6) apparently define an even more potassic critical end point at $\sim An_3Ab_{47}Or_{50}$.

Rocks with relatively K_2O-poor bulk compositions (Group I) crystallized a single feldspar over the whole crystallization range. In sample 1 this feldspar is continuously zoned from $\sim An_{70}$ through anorthoclase compositions to $\sim An_4Ab_{46}Or_{50}$. This single feldspar trend to such potassic rims suggests that the fractionation trend was towards a relatively potassic low-temperature melting composition. It is suggested that the presence of mafic components is responsible for displacing this low melting composition to a more K_2O-rich composition than that of the "phonolite" minimum in the residua system.

Acknowledgements. We thank D.A. Plant and T.C. Hopkins for help in carrying out the energy dispersive microprobe analyses and Dr. R. Kanaris-Sotiriou for the XRF analyses. Professor W.S. MacKenzie and Dr. D.L. Hamilton made many improvements to an earlier version of the paper. A research grant from N.E.R.C. is gratefully acknowledged.

References

Bowen NL, Schairer JF (1938) Crystallization equilibrium in nepheline-albite-silica mixtures with fayalite. J Geol 46:397–411

Brown FH (1970) Zoning in some volcanic nephelines. Am Mineral 55:1670–1680

Carmichael ISE (1964) Natural liquids and the phonolitic minimum. J Geol 4:55–60

Carmichael ISE, Turner FJ, Verhoogen J (1974) Igneous petrology. McGraw-Hill, New York

Dollase WA, Thomas WM (1978) The crystal chemistry of silica-rich, alkali-deficient nepheline. Contrib Mineral Petrol 66:311–318

Greig JW, Barth TFW (1938) The system $Na_2O \cdot Al_2O_3 \cdot 2SiO_2$ (nephelite, carnegieite)-$Na_2O \cdot Al_2O_3 \cdot 6SiO_2$ (albite). Am J Sci 35A:93–112

Gibb FGF, Henderson CMB (1978) The petrology of the Dippin sill, Isle of Arran. Scot J Geol 14:1–27

Hamilton DL (1961) Nephelines as crystallization temperature indicators. J Geol 69:321–329

Hamilton DL, MacKenzie WS (1965) Phase-equilibrium studies in the system $NaAlSiO_4$ (nepheline)-$KAlSiO_4$ (kalsilite)-SiO_2-H_2O. Mineral Mag 34:214–231

Henderson CMB, Gibb FGF (1972) Plagioclase-Ca-rich-nepheline intergrowths in a syenite from the Marangudzi complex, Rhodesia. Mineral Mag 38:670–677

Henderson CMB, Gibb FGF (1977) Formation of analcime in the Dippin sill, Isle of Arran Mineral Mag 41:534–437

Kim K-T, Burley BJ (1971) Phase equilibria in the system $NaAlSi_3O_8$-$NaAlSiO_4$-H_2O with special emphasis on the stability of analcite. Can J Earth Sci 8:311–337

Lindsley DH, Smith D (1971) Chemical variations in the feldspars. Carnegie Inst Washington Yearb 69:274–278

MacKenzie WS (1972) The origin of trachytes and syenites. Progr Expt Petr (NERC) 2:46–50

Mohammed ARO (1982) Mineralogy and petrology of Eilean Mhuire, Shiant Isles. Unpubl Ph D thesis, Univ of Cambridge

Morse SA (1980) Basalts and phase diagrams. Springer-Verlag, Berlin, Heidelberg, New York

Nash WP, Carmichael ISE, Johnson RW (1969) The mineralogy and petrology of Mount Suswa, Kenya. J Petrol 10:409–439

Norris G (1973) Phase relations in petrogeny's residua system with the addition of anorthite. Unpubl Ph D thesis, Univ of Manchester

Parsons I, Brown WL (1983) A TEM and microprobe study of a two-perthite alkali gabbro: implications for the ternary feldspar system. Contrib Mineral Petrol 82:1–12

Roux J, Hamilton DL (1976) Primary igneous analcite – an experimental study. J Petrol 17:244–257

Saha P (1959) Geochemical and X-ray investigation of natural and synthetic analcites. Am Mineral 44:300–313

Schairer JF (1957) Melting relations of the common rock-forming oxides. J Am Ceram Soc 40:215–235

Schairer JF, Yoder HS Jr (1960) The nature of residual liquids from crystallization, with data on the system nepheline-diopside-silica. Am J Sci 258A:273–283

Schairer JF, Yoder HS Jr (1961) Crystallization in the system nepheline-forsterite-silica at 1 atmosphere pressure. Carnegie Inst Washington Yearb 60:141–144

Stewart DB, Roseboom EH Jr (1962) Lower temperature terminations of the three-phase region plagioclase-alkali feldspar-liquid. J Petrol 3:280–315

Thompson RN, MacKenzie WS (1967) Feldspar-liquid equilibria in peralkaline acid liquids: an experimental study. Am J Sci 265:714–734

Tilley CE (1959) A note on the nosean phonolite of the Wolf Rock, Cornwall. Geol Mag 96:503–504

Tuttle OF, Bowen NL (1958) Origin of granite in the light of experimental studies in the system $NaAlSi_3O_8$-$KAlSi_3O_8$-SiO_2-H_2O. Mem Geol Soc Am 74

Accepted August 8, 1983